Neural Identification of SSSC Based on Average model Using GAMMA, DNN, RBF and MLP for Steady State Calculations

M. Tavakoli Bina *Senior Member, IEEE*, A. Houshmand Viki, and S. Rahimzadeh

Abstract-- **The use of exact model of FACTS devices in steady state calculations is complex, due to their switching behavior. However, applying very simple models such as pure inductor/capacitor for FACTS devices leads to inaccurate results in power system studies. In addition in a power market the use of inaccurate models for power system components affects the electrical energy pricing system; while this is very crucial when FACTS devices are used for congestion management of the transmission systems. Average technique provides an appropriate time-domain representation of FACTS devices in which high frequency switching ripples are vanished. But average model can not be directly applied to the power system steady states. Thus this paper extends average model and presents an *average-neural* model of SSSC as a series FACTS device, which is well-suited for analytical purposes in power system applications. To this extend, design and development of four neural identifiers are performed using the GAMMA, DNN, RBF and MLP. To verify the developed models, the exact solutions obtained from the average model of SSSC are compared with the outcomes of the identifiers.**

Keywords: **Averaging technique, FACTS devices, Modeling, Neural network.**

I. INTRODUCTION

THE use and analyze of power electronic devices (e.g. FACTS devices) in power flow studies are complex, due to their switching behavior. Thus it is needed to apply simpler models which are suitable for steady state calculations.

Typically, in [1]-[6], FACTS devices are suggested to alleviate the congestion of transmission systems. The authors in these studies apply pure inductor/capacitor or independent voltage/current source models for FACTS devices. However, power losses of FACTS devices are not included in the analysis by the introduce models, assuming negligible energy consumption by the device itself. When the number and capacity of the employed FACTS devices increases, considerable energy losses is cancelled in power flow analysis (i.e. part of the network load is cancelled). This undermines the correctness of the process of energy pricing system by using inaccurate models for FACTS devices. In other word the more accurate are the developed models, the fairer pricing condition is established. One common method to the modeling of FACTS devices is averaging technique [7]-[8]. Averaging

technique approximates the behavior of discontinuous system by a continuous-time model. The average model appropriately takes into account the low-frequency variations of the DC link of the converter as well as the power losses related to the AC-side. This help to fair pricing of electrical energy in a power market as well as correctness of the results of an optimal placement problem of FACTS devices.

Although the obtained average model of a device is simpler to analyze and easier to apply to the system under steady state conditions, but it can not be directly used for power flow studies. The problem with this model is that it is necessary to solve a set of differential equations for every operating condition, while this is a quite sophisticated process for an Optimal Power Flow (OPF). The problem of the average model can be removed and the model can be applicable by employing of a suitable neural network identifier. A neural network based on the averaging technique can extract a Power Injection Model (PIM) of a FACTS device. Therefore this paper presents four average-neural (AN) models for a Static Synchronous Series Compensator (SSSC) as a series FACTS device which is used for managing of the congestion of transmission systems [1]-[2]. The resultant models produce the required PQ-phasor that is suitable for power system steady states. The neural network identifiers which are applied to average model of SSSC include the GAMMA, Dynamic Neural Network (DNN), Radial Basis Function (RBF) and Multi Layer Perceptron (MLP). The structure of the models is presented and their accuracies are compared. Then the most accurate and reliable AN model is introduced.

II. AVERAGE MODEL OF SSSC

Averaging technique is a common approach to the modeling of power converters [7]-[8]. Switch-mode converters have a discontinuous behavior which is analytically very complex. Average modeling appropriates the behavior of the converter from a periodic discontinuous system to a periodic continuous one maintaining smooth waveforms by removing high order harmonics. Average model of SSSC is shown in Fig. 1(a). In this model, L introduces the equivalent coupling inductance between the converter and the power system. The resistance R is part of the compensator losses concern with the interconnection of the converter to the power system. The other part of the power losses corresponds to the converter losses that are absorbed by the proper modulation of the converter switches. Fig. 1(b) shows typical SSSC power losses in P.U. against the phase shift between the converter

M. Tavakoli Bina is with K. N. Toosi University of Technology, PO Box 16315-1355, Tehran, Iran (e-mail: tavakoli@ieee.org).

output and the power system voltage (α) that is obtained by the average model. While the average model presents a time-dependent circuit, a PQ or PV model is essential for power flow analysis. Hence, here it is performed adaptive analysis to get the supplied active and reactive powers of SSSC. A new bus is added for every SSSC as the converter AC voltage, which is located in an existing transmission line n through the communication reactance (X_{CON}) and the AC resistance (R), see Fig. 2.

III. IDENTIFICATION OF THE AVERAGE MODEL USING NEURAL NETWOKS

Average model which is presented in Fig. 1(a), is identified by using it as a reference to generate required training data for the AN model. Training data are produced so that the operating range of SSSC would be covered. Therefore magnitude of the terminal voltage is varied within $|V_t| \in [0, 0.5]$ P.U. by small steps of 0.01 P.U. and phase angle α ($\angle(V_{CON} - V_t)$) is also varied within $\alpha \in [-1.5^o, 1.5^o]$ by steps of 0.01^0 (see Fig. 2). The sum of steady state operating points to train the neural models is equal to 15000 set.

The time-domain model of Fig. 1(a) is solved for every operating point to reach steady state solution. Then, this is used to calculate and store the absorbing active as well as generating/absorbing reactive powers of SSSC delivered to line n. This leads to construction of database of SSSC operating phasors.

The set of produced training data is applied to four well-known neural networks; GAMMA, RBF, DNN and MLP to find out which of them is suitable. The best neural model is introduced as the AN identifier of SSSC.
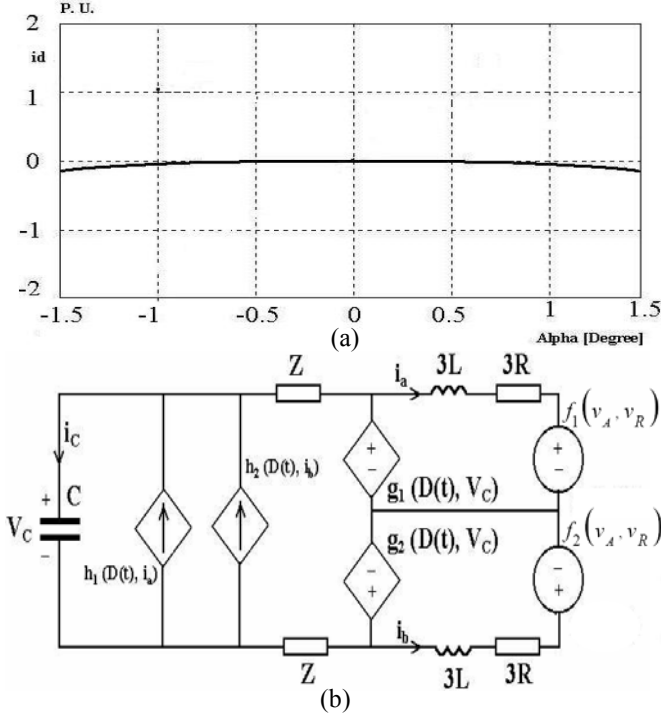

(a)

(b)

Fig. 1. (a) Average circuit model of SSSC, (b) typical internal power losses of SSSC obtained by the average model

A. The GAMMA neural identifier

Figure 3 presents the designed GAMMA neural network for the average model, having two inputs and one output. This designed network includes an input layer, a hidden layer with non-linear neuron functions along with a linear function output layer. Memory size of the GAMMA is determined by the parameter μ. The inputs u_1 and u_2 are separately multiplied by μ, and then passed through a delay block Z^{-1} to arrange memory or filter for the neural network (blocks μ, Z^{-1} and $1-\mu$). Every synapse of the GAMMA network may contain more than one filter, which needs to be determined by designing the structure of the neural network. The lower is the parameter μ, the history of the neural network influences more effectively the generation of the progressing output. Furthermore, synapses may have several weighting factors to improve the capability of modeling nonlinear systems. To show the performance of this neural network, the feed forward calculation using the parameters of Fig. 3 is presented as follows:

$$X_{i1}^1(t) = u_i(t) \tag{1}$$

$$X_{i2}^1(t) = \left(1 - \mu_{i1}^1\right)X_{i2}^1(t-1) + \mu_{i1}^1 X_{i1}^1(t-1) \tag{2}$$

$$X_{i3}^1(t) = \left(1 - \mu_{i1}^1\right)X_{i3}^1(t-1) + \mu_{i1}^1 X_{i2}^1(t-1) \tag{3}$$

$$y_i^1(t) = w_{i1}^1 X_{i1}^1(t) + w_{i2}^1 X_{i2}^1(t) + w_{i3}^1 X_{i3}^1(t) = \sum_{j=1}^3 w_{ij}^1 X_{ij}^1 \tag{4}$$

$$o_i^1(t) = \tan sig\left(y_i^1(t)\right) \tag{5}$$

$$X_{i1}^2(t) = o_i^1(t) \tag{6}$$

$$X_{i2}^2(t) = \left(1 - \mu_{i2}^2\right)X_{i2}^2(t-1) + \mu_{i2}^2 X_{i1}^2(t-1) \tag{7}$$

$$X_{i3}^2(t) = \left(1 - \mu_{i2}^2\right)X_{i3}^2(t-1) + \mu_{i2}^2 X_{i2}^2(t-1) \tag{8}$$

$$y_i^2(t) = w_{i1}^2 X_{i1}^2(t) + w_{i2}^2 X_{i2}^2(t) + w_{i3}^2 X_{i3}^2(t) = \sum_{j=1}^3 w_{ij}^2 X_{ij}^2 \tag{9}$$

$$y(t) = y_1^2(t) + y_2^2(t) = \sum_{i=1}^2 y_i^2(t) \tag{10}$$
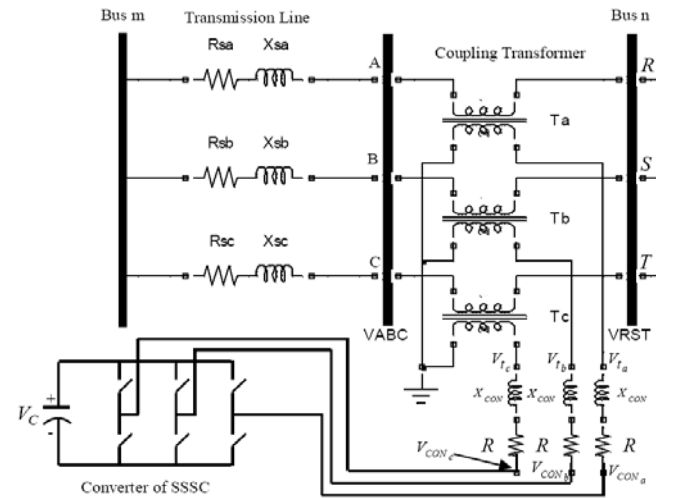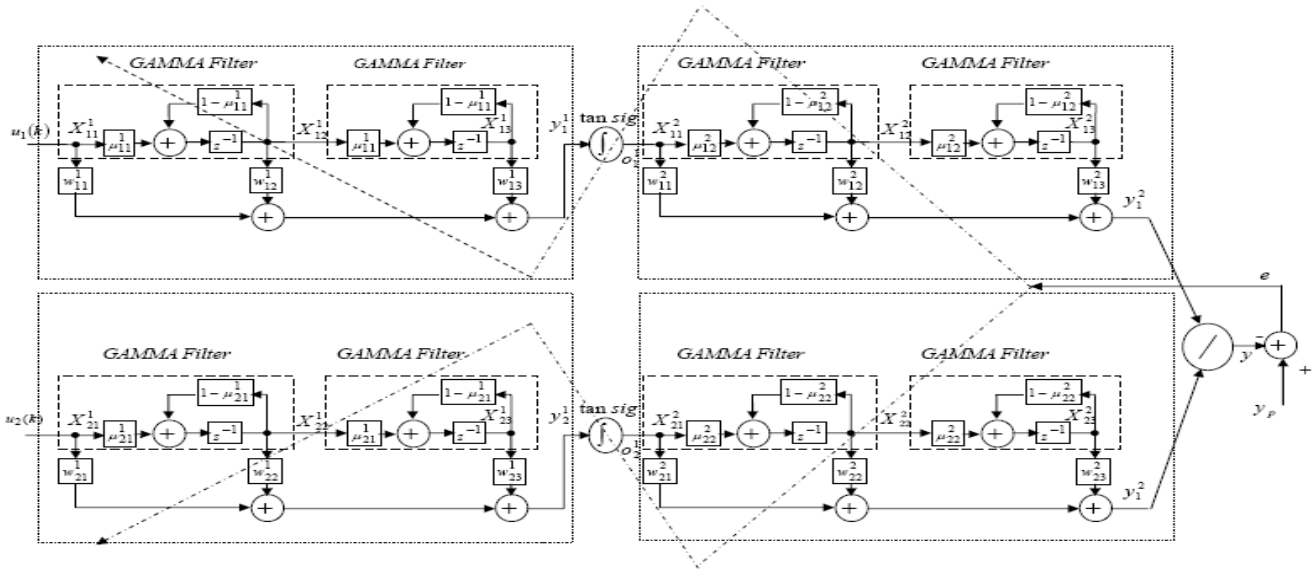

Fig. 2. Three-phase circuit of SSSC

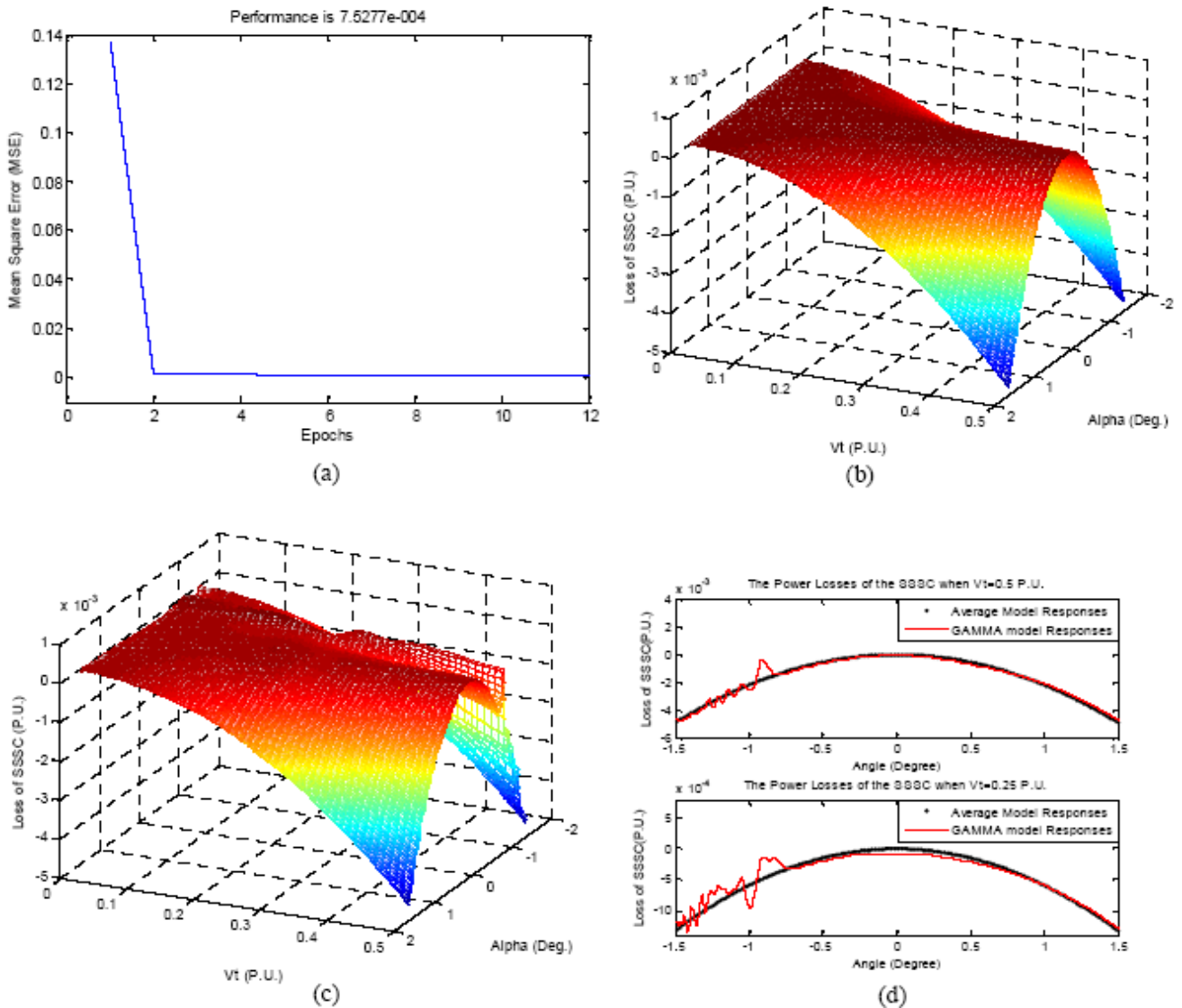Fig. 3. The designed structure of the GAMMA neural network.

Fig. 4. (a) The MSE of the trained data, (b)-(c) Power losses of the exact average model and GAMMA identifier output for 15000 trained data, (d) The output of SSSC when $|V_t| = 0.50$ and 0.25 P.U.

Where the superscript indexes indicate the layer number, the first subscript indexes show the neuron number and the second one introduces the filter number, y is the output of each layer, and w is the weighting factor. The training of the above network can be performed using the back propagation method. Various structures of the GAMMA neural network were examined in this research. Amongst them, a two–layer structure provides the lowest error for the average model of SSSC. Each layer includes 40 GAMMA filters with identical parameters $\mu = 0.9$. Also, the inputs u_1 and u_2 are V_t and reactive power injected to the transmission line (see Fig. 2), and the output y is the power losses of SSSC. Figure 4(a) shows the reduction of mean squared error (MSE) of the trained data, and Figs. 4(b)-(c) depict the exact average model and the output y (power losses) obtained by GAMMA identifier respectively. By increasing V_t, the absorbed power losses of SSSC are also increased.

To examine the capability of the GAMMA network to identify the AN model, Fig. 4(d) zooms in the Figs. 4(b)-(c) for two terminal voltages over $\alpha \in [-1.5^o, 1.5^o]$; $|V_t| = 0.50$ P.U. and $|V_t| = 0.25$ P.U. The exact power losses taken from the average model conform to those of Fig. 1(b) that is reported in [8] and simulated here for SSSC. The GAMMA neural network response corresponds to the output of the developed AN model. The mean error is equal to 1.5134%, and the mean squared error is 0.0752%. It can be seen that the identification of the average model by the GAMMA neural network differs from that of the exact response, providing some unacceptable results. Specifically, the initial trained data introduce bigger errors compared to those of the final errors, because the GAMMA neural network needs the history of operation of SSSC.

B. The DNN neural identifier

There are various structures for the dynamic neural network. The employed structure for identifying the AN model is given by Fig. 5 in which the DNN includes two layers. The hidden layer has delay blocks taken from the neurons, which take the data history of the network into account for the progressing output. Index e corresponds to the exhibitory positive classes (e.g. positive input vector X_e), and index i relates to inhibitory negative classes (e.g. negative input vector X_i). Each neuron from the exhibitory class has a delayed input from its corresponding neuron in inhibitory class and vice versa. Output of each neuron is applied to a non-linear neuron activation function to be able to model non-linear systems. Then, the outcomes of the activation functions are weighted by a^2 for exhibitory classes, and by b^2 for inhibitory classes. These weighted productions are eventually applied to the linear activation function of the output layer to get the output of the DNN. The advantages of the DNN are non-linear modeling capability as well as the fast network convergence because of the inherit delays of the structure. The following relationships describe the designed feed forward state of the network:

$$X_e = [X_e^1 \quad X_e^2]^T \quad , \quad X_i = [X_i^1 \quad X_i^2]^T \tag{11}$$
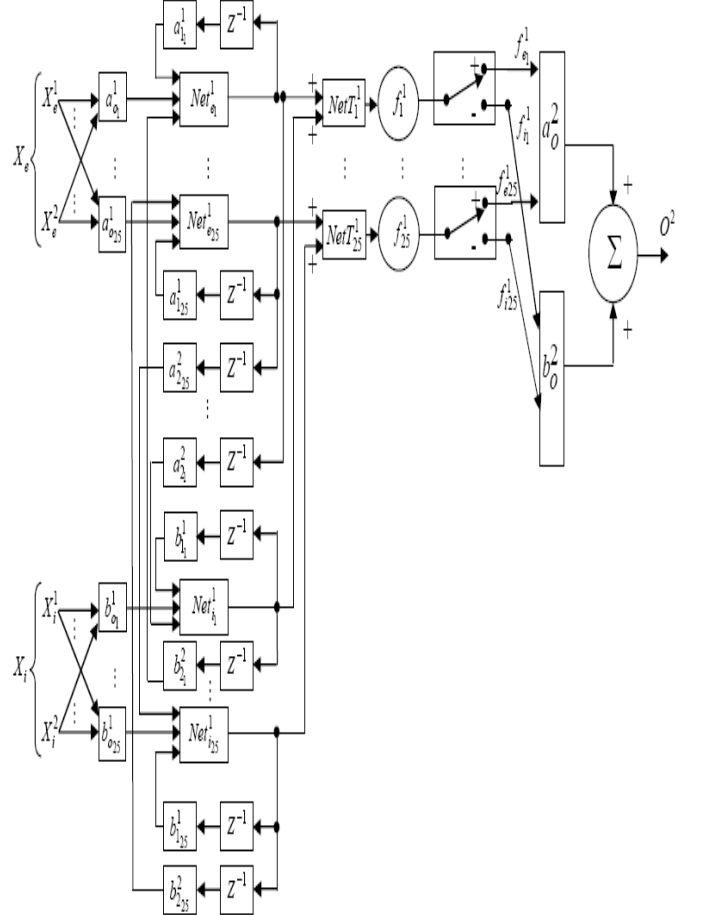

Fig. 5. The structure of the DNN that is designed to identify the average model of SSSC.

$$net_e^1(t) = [net_{e1}^1 \quad net_{e2}^1 ... net_{e25}^1]^T \tag{12}$$

$$net_i^1(t) = [net_{i1}^1 \quad net_{i2}^1 ... net_{i25}^1]^T \tag{13}$$

$$net_{e_j}^1(t) = a_{o_j}^1 X_e^1(t) + a_{o_j}^1 X_e^2(t) + a_{1_j}^1 net_{e_j}^1(t-1) - b_{2_j}^1 net_{i_j}^1(t-1) \tag{14}$$

$$net_{i_j}^1(t) = b_{o_j}^1 X_i^1(t) + b_{o_j}^1 X_i^2(t) + b_{1_j}^1 net_{i_j}^1(t-1) - a_{2_j}^1 net_{e_j}^1(t-1) \tag{15}$$

$$netT_j^1(t) = net_{e_j}^1(t) + net_{i_j}^1(t) \tag{16}$$

$$O_j^1(t) = f_j^1(t) = \frac{1 - e^{-netT_j^1(t).k}}{1 + e^{-netT_j^1(t).k}} \tag{17}$$

$$O^2(t) = \sum_{j=1}^{25} (a_{o_j}^2 f_{e_j}^1(t) + b_{o_j}^2 f_{i_j}^1(t)) \tag{18}$$

where:

$$a_o^2 = [a_{o_1}^2 \cdots a_{o_{25}}^2] \; , \; b_o^2 = [b_{o_1}^2 \cdots b_{o_{25}}^2]$$

$$f_e^1 = [f_{e_1}^1 \cdots f_{e_{25}}^1]^T \; , \; f_i^1 = [f_{i_1}^1 \cdots f_{i_{25}}^1]^T$$

$$f_{e_j}^1(t) = \begin{cases} f_j^1(t) & f_j^1 \geq 0 \\ 0 & f_j^1 \prec 0 \end{cases} \quad , \quad f_{i_j}^1(t) = \begin{cases} f_j^1(t) & f_j^1 \prec 0 \\ 0 & f_j^1 \geq 0 \end{cases}$$

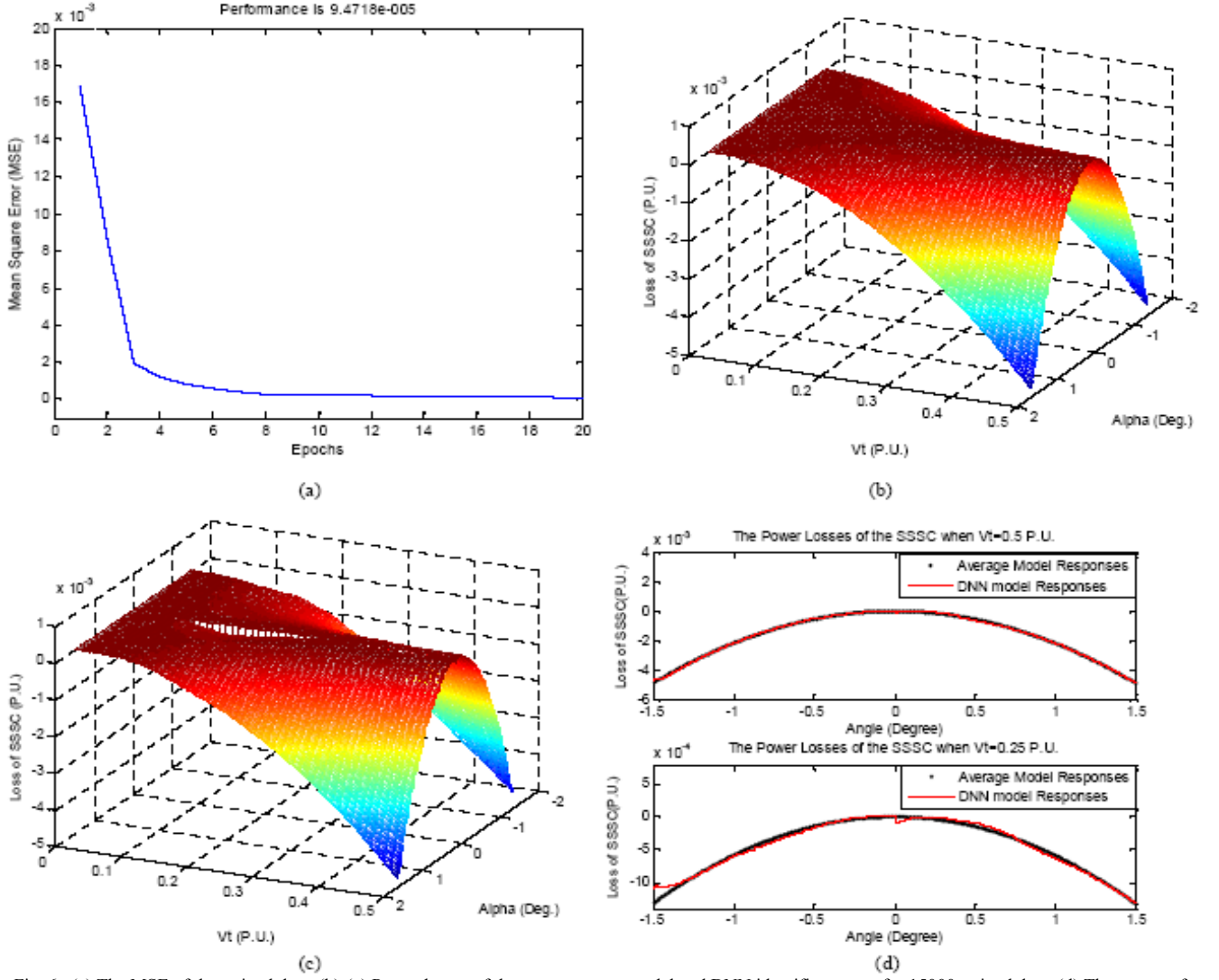$$j = 1, 2, ..., 25$$

(a)

(b)

(c)

(d)

Fig. 6. (a) The MSE of the trained data, (b)-(c) Power losses of the exact average model and DNN identifier output for 15000 trained data, (d) The output of SSSC when $|V_t| = 0.50$ and 0.25 P.U. .

All parameters of the network are trained using the back propagation method, and the structure is designed by trial end error. In this research, different structures were examined in which 25 neurons is considered for the hidden layer alongside with one neuron for the output layer.

Figure 6(a) shows the reduction in mean squared error of the training data, Figs. 6(b)-(c) depict the power losses analyzed by the average model as well as the output of the DNN. Figure 6(d) zooms in Figs. 6(b)-(c) for two terminal voltages over $\alpha \in [-1.5^o, 1.5^o]$; $|V_t| = 0.50$ P.U.and $|V_t| = 0.25$ P.U. Simulation results indicate that the AN model of SSSC, developed by the DNN, introduces the mean squared error of 0.0095% and mean error of 0.6657% for the trained data. This situation confirms that the DNN is unable to develop successfully the AN model of SSSC because the DNN uses the history of the response to identify the progressing output.

C. The RBF neural identifier

The designed RBF neural network is illustrated by Fig. 7, having two input vectors (X_1, X_2) and one output (y). The inputs are applied directly to the neurons with Gaussian activation functions as follows:

$$\Phi_i(r) = e^{-\frac{r_i^2}{2\sigma^2}} \qquad \sigma \succ 0, \quad r_i = \|X - t_i\| \qquad (19)$$

$\|X - t_i\| =$ distance of $X = [X_1, X_2]$ from vector t_i (20)

Where t_i and σ_i are the centre and spread of the Gaussian function Φ_i, and r_i is the Euclidean distance of X from t_i.
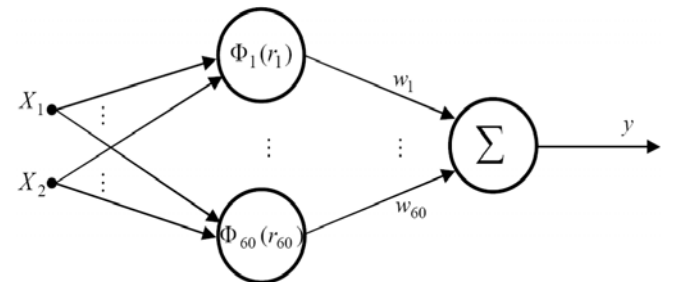

Fig. 7. Designed schematic structure of the RBF neural network to identify average model of SSSC.
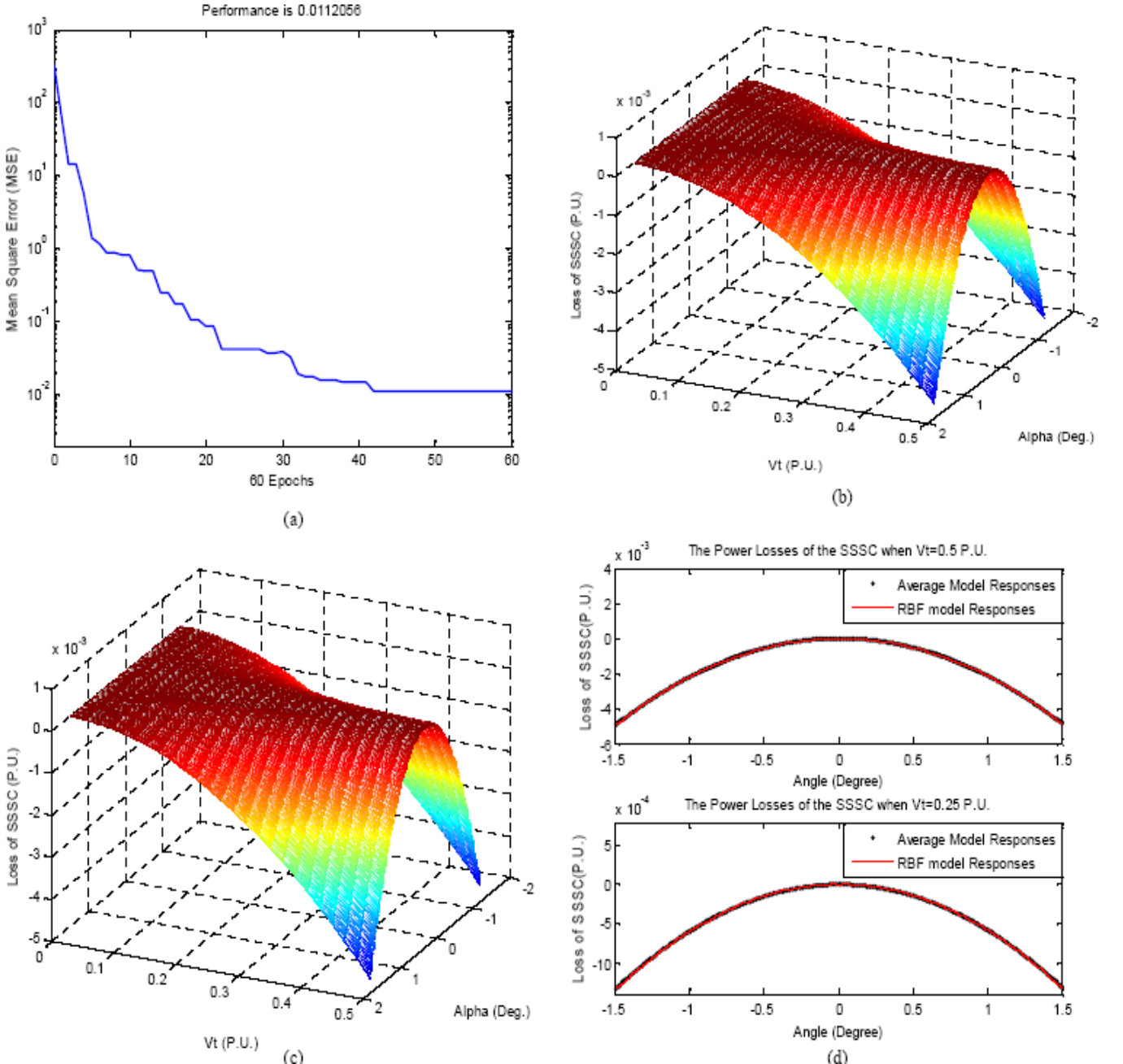
Fig. 8. (a) The MSE of the trained data, (b)-(c) Power losses of the exact average model and RBF identifier output for 7500 trained data, (d) The output of SSSC when $|V_t| = 0.50$ and 0.25 P.U. .

The output y of the designed neural network can be given by applying sixty weighting factors (w_i for $i = 1, \cdots, 60$) to the activation functions:

$$Y = w_1 \Phi_1 (\|X - t_1\|) + \dots + w_{50} \Phi_{50} (\|X - t_{50}\|) \quad (21)$$

To classify the data of the average model of SSSC, the Euclidean distance of all 15000 training data from each other are needed to be calculated and stored. This necessitates huge memory space for the neural network, forcing the program to double the steps of V_t . This lowers the number of training data to 7500. The number of neurons of the hidden layer is set to

60 by trial and error. The spread of Gaussian functions is designed to be equal to one.

Figure 8(a) shows total squared error of the training data, where the mean error and mean squared error are equal to 0.0907% and 0.0149% respectively, and Figs. 8(b)-(c) illustrates the power losses of SSSC produced by the average model for 7500 steady state operating conditions as well as the response of the RBF neural network. To discuss the suitability of the RBF for the AN model, Fig. 8(d) zooms in the Figs. 8(b)-(c) for two terminal voltages over $\alpha \in [-1.5^o, 1.5^o]$; $|V_t| = 0.50$ P.U. and $|V_t| = 0.25$ P.U.
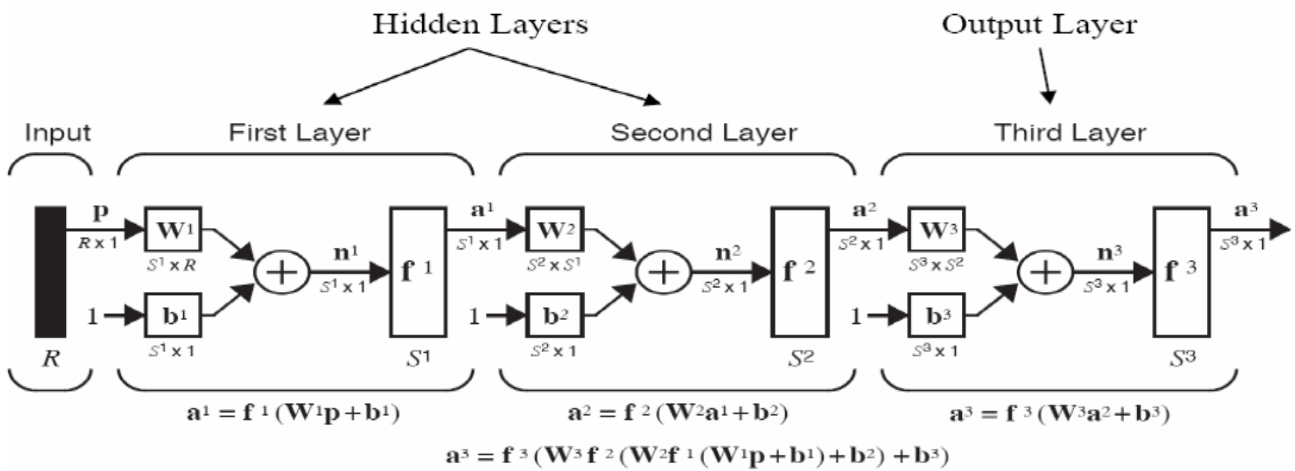
Fig. 9. The structure of the designed MLP neural network to identify the average model of SSSC.
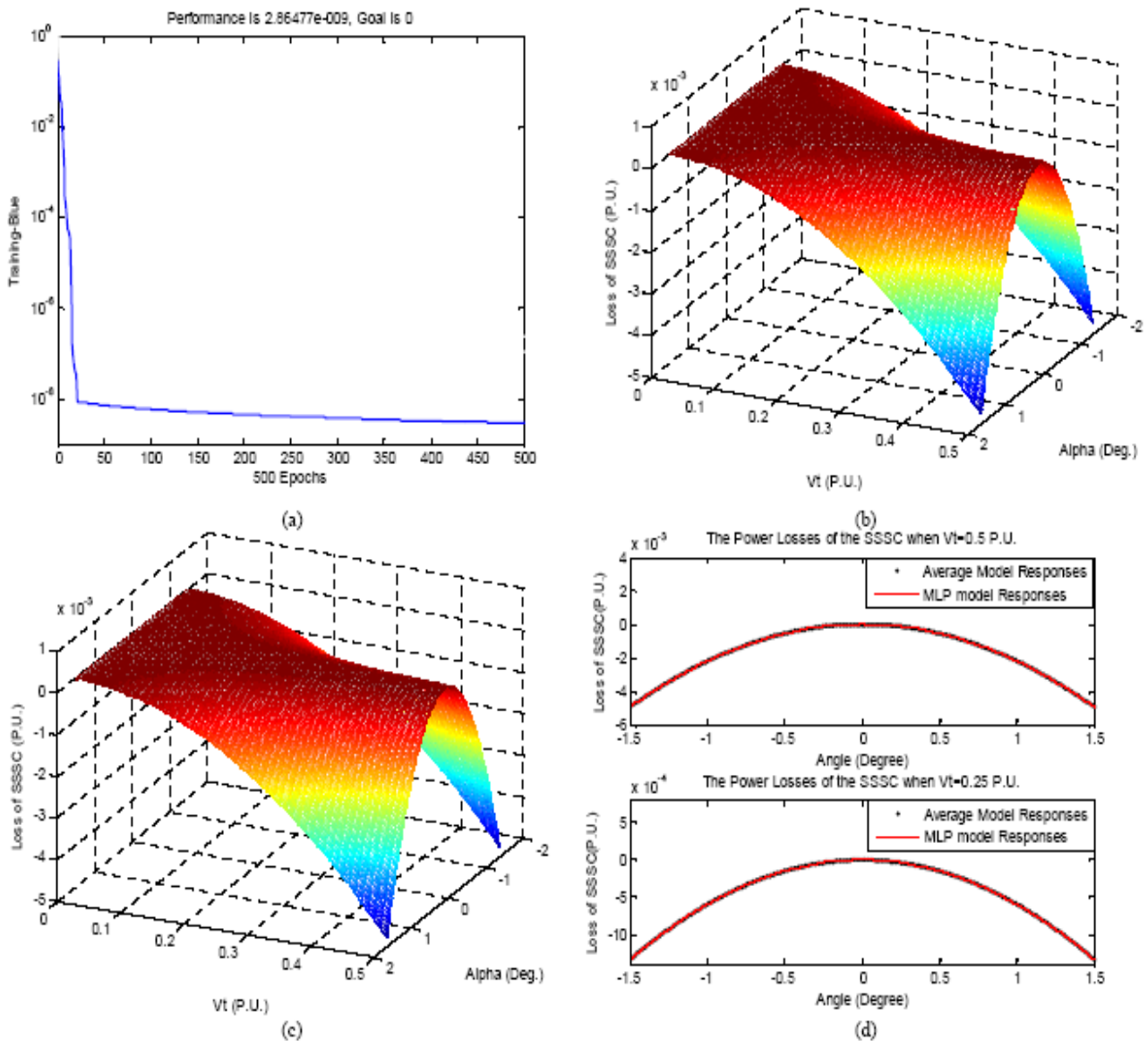

Fig. 10. (a) The MSE of the trained data, (b)-(c) Power losses of the exact average model and MLP identifier output for 15000 trained data, (d) The output of SSSC when $|V_t| = 0.50$ and 0.25 P.U. .

D. The MLP neural identifier

The MLP neural network is a global estimator, which an initial processing on training data is taken place followed by designing its structure for the AN model. Structure of this design is shown by Fig. 9, where three hidden layers are proposed for the MLP neural network. By examining and performing various tests, twelve neurons are considered for the first and the second layers and one neuron for the third layer. Neuron functions of the first and the second layers are considered identical as follows:

$$f^1(n) = f^2(n) = \frac{e^n - e^{-n}}{e^n + e^{-n}} \tag{22}$$

Also, weighting matrices of the three layers are W^1, W^2 and W^3, and the 2×1 input vector P includes the terminal voltage and injected reactive power of SSSC to transmission line as shown by Fig. 2. Three vectors b^1, b^2 and b^3 are the threshold values of the neurons, and three outputs of the three layers are a^1, a^2 and a^3. To train this network, again 15000 operating states are used. Figure 10(a) demonstrates the reduction of the mean squared error during the training process and Figs. 10(b)-(c) give the exact power losses of the average model and the response of the MLP AN model. Figure 8(d) zooms in the Figs. 8(b)-(c) for two terminal voltages over $\alpha \in [-1.5^o, 1.5^o]$; $|V_t| = 0.50$ P.U. and $|V_t| = 0.25$ P.U. Simulation results show that when the AN model of SSSC is identified by the MLP, then the error between the average and the AN models is considerably low. The mean error is equal to 0.0033%, and the mean squared error is 0.000000286%.

Now it is easy to compare each identifier with the other identifiers of the average model of SSSC. It should be noted, however, that the error of the RBF method is calculated for 7500 trained data whereas the other identifiers take 15000 trained data into account. Hence, the MLP identifies the average model with an acceptable error, much lower than three other neural network identifiers.

In [9] a lossless current-based model for the SSSC is introduced which due to eliminating of the losses, the model has about 3% error on the basis of SSSC capacity. But the proposed model in this paper takes the losses of SSSC into account and the related error is removed.

IV. CONCLUSION

Averaging modeling approximates a discontinuous complex system to a simple continuous structure, preserving the original characteristics such as DC-link voltage variations related to power losses and modulation index. Thus, the average model of SSSC is more suitable for power system analysis (e.g. the OPF) compared to its conventional simple capacitive/inductive model. This paper considers the previously introduced average model of SSSC in the time domain. It is proposed that the time domain variables can be treated using the neural network identifier to achieve frequency domain power system phasors. Hence, the GAMMA, DNN, RBF and the MLP neural networks are used to identify the SSSC in steady states. These four networks are trained using simulation of the average model up to 15000 steady-state operating conditions. Further, outcomes of the developed AN models are compared with simulations of the exact average model. Then, advantages as well as disadvantages of both identifiers are examined, and the resultant errors are compared.

V. REFERENCES

[1] Muwaffaq I. Alomoush, "Static Synchronous Series Compensator to Help Energy Markets Resolve Congestion-Caused Problems," *Large Engineering systems Conference on Power Engineering,* Canada , 28-30 July 2004, pp. 25 - 29.
[2] R. Mihalic, "Power Flow Control with Controllable Reactive Series elements," *IEE Proc.-Gener. Transm. Distrib.*, Vol. 145, No. 5, Sep. 1998, pp. 493-498.
[3] Sergio Bruno, Massimo La Scala, "Unified Power Flow Controllers for Security-Constrained Transmission management," *IEEE Transactions on Power Systems*, Volume 19, Issue 1, Feb. 2004, pp. 418- 426.
[4] A.Berizzi, Maurizio Delfanti, Paolo Marannino, Marco Savino Pasquadibisceglie, Andrea Silvestri, "Enhanced Security-Constrained OPF with FACTS Devices," *IEEE Trans. On Power Systems*, Vol.20, NO.3, Aug. 2005, pp. 1597-1605.
[5] L.Ippolito, P. Siano, "Selection of Optimal Number and Location of Thyristor-Controlled Phase Shifters Using Genetic Based Algorithms," *IEE Proc.-Gener. Transm. Distrid.*, Vol. 151, No. 5, Sep. 2004, pp. 630-637.
[6] Ying Xiao, Y. H. Song, Chen-Ching Liu and Y. Z. Sun, "Available Transfer Capability Enhancement Using FACTS Devices," *IEEE Trans. On Power Sys.* , Vol. 18, No. 1, Feb. 2003, pp. 305-312.
[7] I.Etxeberria-Otadui, V.Manzo, S.Bacha, F.Baltes, "Generalized Average Modelling of FACTS for Real Time Simulation In ARENE," *IEEE 2002 28th Annual Conference of the Industrial Electronics Society, IECON 02*, Vol. 2, 5-8 Nov., pp. 864-869.
[8] M. Tavakoli Bina, D.C. Hamill, "Average circuit model for angle-controlled STATCOM," *IEE Proc.-Electr. Power Appl.*, Vol. 152, No. 3, May 2005, pp. 653-659.
[9] A. Vinkovic, R. Mihalic, "A current-based model of the static synchronous series compensator (SSSC) for Newton-Raphson power flow ," *EPSR*, Vol. 78, May 2008, pp. 1806-1813.

VI. BIOGRAPHIES

M. Tavakoli Bina was born in Tehran, Iran, on July 14, 1962. He received a B.Sc. degree from the University of Teheran in 1992, and his Ph.D. degree in power electronics and power system interconnection from the University of Surrey in the UK in June 2001. He has been an IEEE member for six years. He is presently holding an associate professor position at the K. N. Toosi University of Technology, researching in the area of designing power electronics devices as well as power system analysis.

A. Houshmand Viki was born in Tehran, Iran, on July 27, 1950. He received a B.Sc. degree from the Amirkabir University of Technology in 1972, MSc. degree in power electric from Bradford University in the UK in 1987, and Ph.D. degree in power electric from Manchester University in the UK in 1990. He joined from 1990 K.N.Toosi University of technology as assistant professor since now. His research area is designing power electronic devices as well as electrical machine controlling systems.

Sajad Rahimzadeh was born in Ilam, Iran on March 21, 1975. He received his B.Sc. and M. SC. degrees from Isfahan University of Technology in 1998 and 2000 respectively. He is now a Ph.D. student at the K. N. Toosi University and his working area is control and modulation of FACTS controllers in application to the electricity market.